CERN – EUROPEAN ORGANIZATION FOR NUCLEAR RESEARCH

CLIC – Note – 1200

PERFORMANCE OPTIMIZATION OF THE CLIC POSITRON SOURCE

Y. Zhao, S. Doebert and A. Latina

CERN, Geneva, Switzerland

CERN-ACC-2024-0005
30/10/2024

Abstract

The baseline configuration of the CLIC positron source is optimized at different center-of-mass energy stages of the collider for different acceleration modes. The hybrid target is replaced with a single amorphous tungsten target with the target thickness and electron beam spot size reoptimized. As a result, the final positron yield accepted by the pre-damping ring is significantly increased, and the electron beam power and total deposited power in the target are significantly reduced. The most realistic start-to-end simulation to date of the target, matching device, pre-injector linac, solenoids, chicane and injector linac are performed taking into account new design of essential hardware. The impact of misalignments was studied for the first time for the CLIC positron source. Possibility for reducing the electron beam energy is investigated.

Geneva, Switzerland
October 2024

Performance Optimization of the CLIC Positron Source

Yongke Zhao,* Steffen Doebert, and Andrea Latina
CERN, Geneva, Switzerland

(Dated: October 30, 2024)

The baseline configuration of the CLIC positron source is optimized at different center-of-mass energy stages of the collider for different acceleration modes. The hybrid target is replaced with a single amorphous tungsten target with the target thickness and electron beam spot size reoptimized. As a result, the final positron yield accepted by the pre-damping ring is significantly increased, and the electron beam power and total deposited power in the target are significantly reduced. The most realistic start-to-end simulation to date of the target, matching device, pre-injector linac, solenoids, chicane and injector linac are performed taking into account new design of essential hardware. The impact of misalignments was studied for the first time for the CLIC positron source. Possibility for reducing the electron beam energy is investigated.

I. INTRODUCTION

The Compact Linear Collider (CLIC) [1, 2] is a multi-TeV high-luminosity linear collider proposed to be built at the border of Switzerland and France, hosted by the European Organization for Nuclear Research (CERN). A novel two-beam acceleration technique with normal conducting X-band accelerating structures has been developed, operating with a high average RF gradient in the range of 70 MV/m to 100 MV/m. The CLIC Conceptual Design Report (CDR) [1] was published in 2012. Three center-of-mass energy stages were proposed: 500 GeV, 1.5 TeV and 3 TeV. However, the CDR was mainly focused on demonstrating the feasibility of the CLIC accelerator at 3 TeV. The CLIC Project Implementation Plan (PIP) report [2] was published in 2018, with high-quality, very detailed documentation of baseline and alternative CLIC configurations. With the discovery of the Higgs boson in 2012, the first energy stage was then optimized and reduced to 380 GeV, which provides an excellent opportunity to perform precision measurements of the Standard Model (SM) physics processes, particularly in the Higgs and top-quark sectors. The higher energy stages provide opportunities to explore TeV-scale phenomena such as the Higgs self-coupling and Beyond Standard Model (BSM) physics.

To achieve the design performance, CLIC needs high-quality electron and positron bunches. This paper focuses on the positron production scheme. The CLIC positron source must provide high-intensity and high-energy positron beams up to 2.86 GeV, which are then injected into the pre-damping ring (PDR). The schematic layout of the optimized baseline design of the CLIC positron source is presented in Fig. 1. Positrons are generated with a 5 GeV electron beam from a thermionic electron gun and a driver linac impinging on a single amorphous tungsten target. The design of the electron gun and driver linac are not studied and discussed in this report. A pulsed tapered flux concentrator (FC) [3] is used as the adiabatic matching device (AMD), with an adiabatically decreasing magnetic field. The pre-injector linac (PIL), composed of L-band traveling wave (TW) RF accelerating structures [4] and 0.5 T surrounding normal-conducting (NC) solenoids, will further capture and accelerate the positrons to about 200 MeV. Electrons and photons from the target are removed by a chicane and a collimator located at the PIL exit. The injector linac (IL) [5], which will be used for both electrons and positrons, will accelerate the positron beam to 2.86 GeV, with quadrupoles and the same L-band TW structures. At the PDR entrance, the longitudinal acceptance for the positron beam is considered by applying energy and time cuts. The PDR accepted positron yield is defined as the ratio of the number of positrons accepted by the PDR to the number of primary electrons.

II. THE CLIC POSITRON SOURCE

The target is simulated with Geant4 [6–8]. In the case of a hybrid target composed of crystal tungsten and amorphous tungsten, Fot [9], a simulation code developed mainly for photon production from the electron channeling process in crystal tungsten, is used. The energy deposition in the target is estimated by creating a 3D cubic mesh around the target, with an optimized mesh grid size of 0.5 mm [10]. The peak energy deposition density (PEDD) is estimated by reading the maximum energy deposition in the mesh, scaled by the material density and the mesh volume. The PEDD is always normalized by the PDR accepted positron yield and the required bunch charge at the PDR entrance. The PEDD in the amorphous tungsten target is usually required to be less than 35 J/g [1]. RF-Track [11, 12] is used to simulate the transport of the positron beam from the target to the PDR entrance.

To simplify the start-to-end simulation and optimization of the entire positron source, an analytic formula is usually used to calculate the energy gain of the positrons

* yongke.zhao@cern.ch

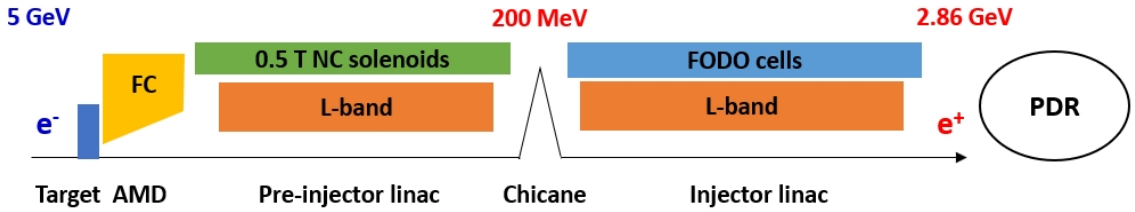

FIG. 1. Schematic layout of the latest baseline design for the CLIC positron source. Electron gun and driver linac are not inlcuded. AMD: Adiabatic Matching Device. FC: Flux Concentrator. PDR: Pre-Damping Ring.

from the PIL exit to the PDR entrance:

$$\Delta E = (2.86\,\mathrm{GeV} - E_{\mathrm{ref}}) \cdot \cos(2\pi f \cdot (t - t_{\mathrm{ref}}))\,, \qquad (1)$$

where, E_{ref} and t_{ref} are the energy and time of the reference particle, which usually need to be optimized for a maximum PDR accepted positron yield, and $f = 2\,\mathrm{GHz}$ is the L-band RF frequency. The time distribution at the PDR entrance in this case is the same as it is at the PIL exit. Such a manner to estimate the PDR accepted positron yield is called the "fast simulation" hereafter. Otherwise, it is called the "full simulation", where all elements are simulated. In the "fast simulation", the chicane is also not simulated, and the magnetic field of the solenoids surrounding the PIL RF structures is replaced with a constant field of 0.5 T where necessary. This makes the "fast simulation" much faster than the "full simulation", but the results are also less realistic and conservative. To be more conservative, when the "fast simulation" is used, the PEDD in the target is required to be less than 30 J/g instead of 35 J/g, taking into account the realistic losses of the positron yield. A comparison between the "fast simulation" and the "full simulation" is summarized in Table I.

TABLE I. Comparison between "fast simulation" and "full simulation".

Configuration	"Fast simulation"	"Full simulation"
NC solenoid	Uniform field	Analytic field
Chicane	Not considered	6D simulation
Injector linac	Analytic (longitudinal)	6D simulation
PEDD limit	30 J/g	35 J/g

A. Beam parameters

The primary electron beam is assumed to have a Gaussian distribution profile in the transverse and longitudinal phase spaces without correlations. The latest baseline parameters of the electron beam and the requirements for the positron beam at the PDR entrance are summarized in Table II, at different energy stages for both drive beam-based (DBA) and klystron-based (KBA) acceleration modes. Each case has specified bunch charge and number of bunches with optimal overall luminosity performance. The electron transverse momentum spread, $\sigma_{P_{x,y}}$, is determined by the normalized transverse emittance, $\epsilon^n_{x,y}$, and the spot size, $\sigma_{x,y}$, which can be expressed with the following equation:

$$\epsilon^n_{x,y} = \frac{\sigma_{x,y} \cdot \sigma_{P_{x,y}}}{m_0 \cdot c}\,, \qquad (2)$$

where m_0 is the electron rest mass. The electron spot size has been optimized to have a maximum PDR accepted positron yield and an acceptable PEDD in the target, as presented in Fig. 2. In the old baseline design and studies, a fixed electron spot size of 2.5 mm was used. The required bunch charge of the primary electrons is determined by the PDR accepted positron yield and the required positron bunch charge at the PDR entrance. After applying the PDR acceptance cuts, a 20% safety margin is considered in the positron bunch population and bunch charge at the PDR entrance, allowing for additional losses for the PDR acceptance.

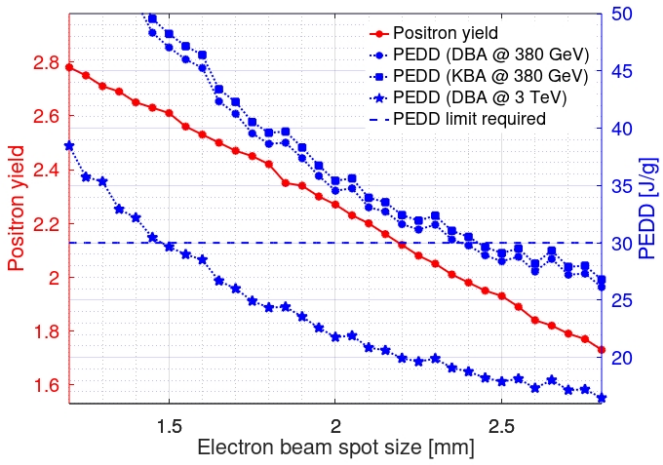

FIG. 2. Scan of the electron beam spot size. PDR accepted positron yield and normalized PEDD at different energy stages for different acceleration modes are plotted as a function of the spot size.

TABLE II. Primary electron beam parameters and requirements for the positron beam at the PDR entrance after applying the PDR longitudinal acceptance cuts at different energy stages for different acceleration modes (DBA: drive beam-based acceleration; KBA: klystron-based acceleration). A 20% safety margin is considered in the positron bunch population and bunch charge.

Beam parameter	Unit	380 GeV		1.5 & 3 TeV
Acceleration mode		DBA	KBA	DBA
Electron beam				
Beam energy	GeV	5	5	5
Energy spread (σ_E/E)	%	0.1	0.1	0.1
Bunch length (σ_z)	mm	1	1	1
Spot size ($\sigma_{x,y}$)	mm	2.40	2.45	1.50
Normalized transverse emittance, $\epsilon^n_{x,y}$	mm·mrad	80	80	80
Number of bunches per train		352	485	312
Positron beam				
Beam energy	GeV	2.86	2.86	2.86
Number of bunches per train		352	485	312
Bunch population without safety margin	10^9	5.200	3.870	3.700
Bunch population with safety margin	10^9	6.240	4.644	4.440
Bunch charge without safety margin	nC	0.833	0.620	0.593
Bunch charge with safety margin	nC	1.000	0.744	0.711
PDR energy acceptance (±)	%	1.2	1.2	1.2
PDR time cut window (total length)	mm/c	20	20	20

B. Target

In the CLIC PIP report published in 2018, a hybrid target has been used, which is composed of a thin crystal tungsten target of 1.4 mm and a thick amorphous tungsten target of 10 mm, with a distance of 2 m. The schematic layout of the hybrid target is displayed in Fig. 3. The crystal target is thought to be able to enhance photon production from the electron channelling process. A dipole with a magnetic field of 0.5 T is placed between the two targets to remove charged particles and reduce the PEDD in the amorphous target, as the PEDD in the amorphous target is usually much higher than the crystal target. In a report published in 2019 [13], the hybrid target has been optimized for a higher positron yield, focusing on the 3 TeV energy stage.

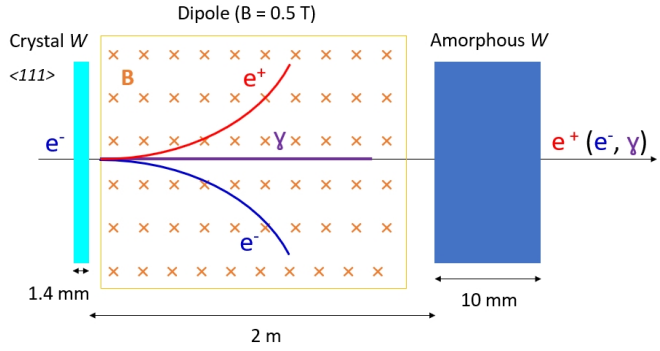

FIG. 3. Schematic layout of the hybrid target in the old baseline design, composed of a thin crystal tungsten and a thick amorphous tungsten. A dipole is supposed to be used between the targets to remove charged particles.

The advantage of using the hybrid target is that it is thought to significantly reduce the PEDD compared with the conventional single amorphous tungsten target. However, we have found that the PDR accepted positron yield of using the hybrid target is much lower than using a single amorphous tungsten target. This is mainly due to the fact that the long distance between the crystal and the amorphous targets leads to a large positron beam size and low transport efficiency to the PDR. A scan of the hybrid target distance is presented in Fig. 4. The PDR accepted positron yield and the normalized PEDD in the amorphous target are estimated and plotted as a func-

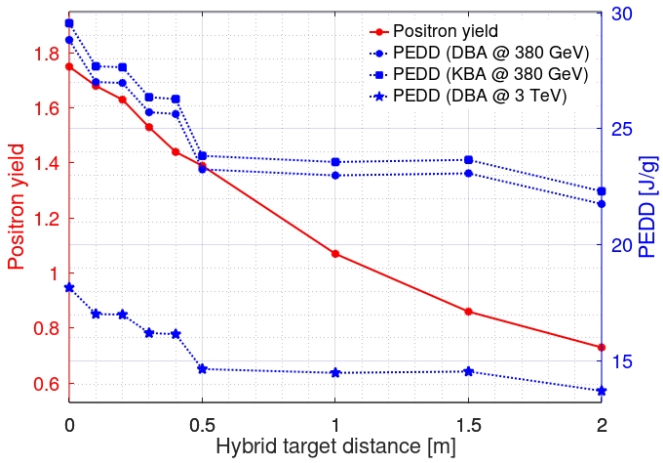

FIG. 4. Scan of the hybrid target distance in the old baseline design. PDR accepted positron yield and normalized PEDD at different energy stages for different acceleration modes are plotted as a function of the distance.

tion of the distance between the crystal and amorphous targets. To simplify the study, the "fast simulation" is used in this case. Clearly it can be seen from the plot that the PDR accepted positron yield is increased significantly with a reduced distance, and the maximum yield is achieved when the distance is zero, which turns out to be a single target option. Even though the PEDD is also increased significantly with a reduced distance, it is still below 30 J/g, and it is possible to reduce the PEDD with an optimized target thickness and increased electron beam spot size. Therefore, in the optimized baseline design, we use a single amorphous target, which gives much higher PDR accepted positron yield than the hybrid target option. Besides, the design, manufacturing and mounting of the target will also be much easier. The schematic layout of the single amorphous tungsten target with an optimized thickness of 18 mm is presented in Fig. 5. The tungsten (W_{74}) has a density of 19.254 g/cm^3 and a melting point of 3,422 °C. A scan of the target thickness is

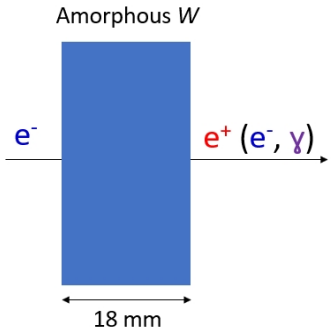

FIG. 5. Schematic layout of the single amorphous tungsten target in the new baseline design, with an optimized thickness of 18 mm.

presented in Fig. 6. The PDR accepted positron yield is

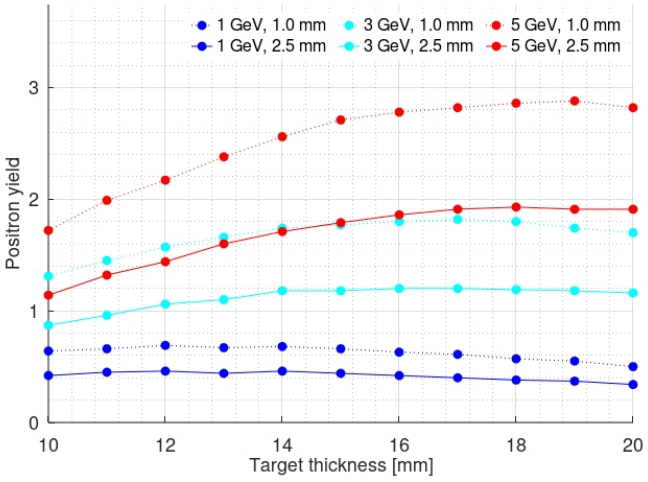

FIG. 6. Scan of the single target thickness in the new baseline design. PDR accepted positron yield is plotted as a function of the thickness for different beam energies and spot sizes.

estimated and plotted as a function of the target thickness for different electron beam energies and spot sizes. At 5 GeV, which is the baseline electron beam energy, the optimized target thickness is about 18 mm.

A comparison of the target configuration and the final results between the old and optimized baselines is summarized in Table III at different energy stages for the DBA acceleration mode. To achieve a fair comparison, the same simulation code is used, and to simplify the study, the "fast simulation" is still used in this case. As a result of optimization, the final positron yield is significantly increased, and the electron bunch charge and beam power are significantly reduced. Compared with the most recently published optimization in 2019, the positron yield has been improved by a factor of 1.65, enabling the same reduction in the bunch charge and beam power of the primary electron beam. The total deposited power in the target is reduced by a factor of 2.1. Compared with the CLIC PIP report published in 2018, which is thought to be a very important roadmap for CLIC construction, the improvements are even more significant, as can be seen in the table. The design, manufacturing and mounting of the new target scheme will also be much easier and conservative.

C. Adiabatic Matching Device

The Adiabatic Matching Device (AMD) is used to capture and improve the transport efficiency of the positrons with large divergence from the target. A strong peak on-axis magnetic field is usually required. The conventional way to achieve this is to use a pulsed normal conducting (NC) flux concentrator (FC) with a tapered inner aperture. The maximum peak on-axis field that can be achieved by a FC is usually thought to be no larger than 6 T due to technical limitations.

In the old studies, the AMD was never designed, and a realistic magnetic field of the AMD was never used. A simple on-axis magnetic field has been assumed, as presented in Fig. 8, which is given by an adiabatic formula [14]:

$$B_z = \frac{B_0}{1 + \mu \cdot z}\,, \tag{3}$$

where, $B_0 = 6$ T is the peak on-axis field and $\mu = 55\,\mathrm{m}^{-1}$ is an optimized scaling factor to shape the field.Besides, in the old studies, a constant inner aperture radius of 20 mm instead of a tapered aperture has been assumed in the simulations, which is not realistic and gives an overestimated positron yield.

In the new baseline and simulations, we use realistic aperture and 2D magnetic field for the AMD. A pulsed FC with a tapered aperture has been designed for the CLIC positron source, based on the SLAC FC design [15], and published earlier in a separate report, as detailed in reference [3]. The inner aperture radius is increased linearly from 6.5 mm at the entrance to 55.45 mm at the

TABLE III. Comparison of the old and optimized target configurations and "fast simulation" results at the 380 GeV energy stage (numbers in parentheses are for 1.5 and 3 TeV energy stages) for the DBA acceleration mode.

Parameter	Unit	PIP report in 2018	Report in 2019	Optimization
Electron beam energy	GeV	5	5	5
Electron beam spot size	mm	2.50	2.50 (1.25)	2.40 (1.50)
Required electron bunch charge	nC	1.37 (0.97)	0.83 (0.39)	0.51 (0.27)
Normalized electron beam power	kW	120.5 (76.0)	73.3 (30.3)	44.4 (21.2)
Target profile		Hybrid	Hybrid	Single
Target thickness	mm	1.4, 10	2.17 (1.68), 17.6 (14.9)	18
Hybrid target distance	m	2	0.67 (0.66)	-
Normalized PEDD in amorphous target	J/g	21.8 (13.7)	24.4 (25.6)	29.8 (29.6)
Normalized deposited power in amorphous target	kW	12.3 (7.7)	25.3 (8.2)	12.0 (5.7)
PDR accepted positron yield	e^+/e^-	0.73	1.20 (1.83)	1.98 (2.61)

exit. The outer radius is 60 mm. The total length of the FC is 127 mm. The gap between the target and the AMD is assumed to be 2 mm. The current is pulsed with a half-sine wave function and a frequency of 25 kHz. The peak current is 20 kA. The schematic layout of the AMD is displayed in Fig. 7. The realistic on-axis magnetic field

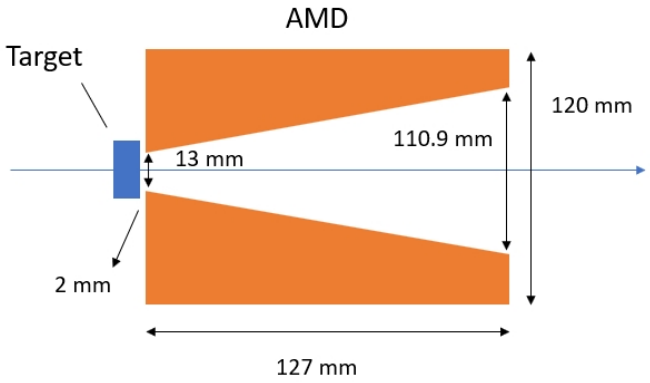

FIG. 7. Schematic layout of the AMD in the new baseline. A FC with a tapered aperture is used as the AMD, placed 2 mm downstream the target.

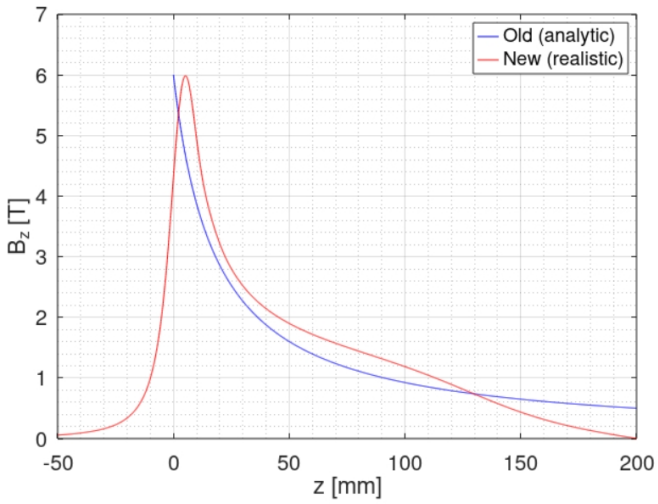

FIG. 8. Comparison between analytic and realistic on-axis magnetic fields of the AMD that are used in the old and new baselines and simulations respectively.

of the AMD is presented in Fig. 8, with a comparison with the analytic field used in old simulations. The prototype of the FC is being manufactured at CERN and is planned to be tested at the KEK test bench.

D. Pre-Injector Linac

The Pre-Injector Linac (PIL) is placed downstream of the AMD, and is used to further capture and accelerate the positrons to about 200 MeV. Similar design of the PIL as in the old studies [13] is used. L-band TW structure [4], which is called the "CLIC L-band" structure, with an RF frequency of 2 GHz and a phase advance per cell of $2\pi/3$, is used. The structure is 1.5 m long and was designed mainly for the CLIC booster linac with a tapered iris radius from 20 mm to 14 mm. However, a constant iris radius of 20 mm is still assumed in our simulations for the positron source. The PIL comprises 11 TW structures and is surrounded by NC solenoids, which are supposed to provide a uniform magnetic field of 0.5 T. To simplify the design, the distance between the structures is assumed to be always 20 cm, although it is found that the positron yield might be slightly increased by reducing the distance between the first two structures. To simplify the simulation and the RF phase optimization, the average RF gradient is assumed to be always 20 MV/m for all RF structures, and two RF phases are used and optimized, one RF phase for the first structure and one RF phase for the other structures.

In the old studies, the layout of the NC solenoids has never been designed and considered. Instead, solenoids were always replaced with an on-axis field of 0.5 T, which is not realistic. In the new simulations, we use the following analytic formula [16] to describe the on-axis magnetic

field of the NC solenoids:

$$B_z = \frac{\mu_0 N I}{2}\left(\frac{l/2-z}{l\sqrt{R^2+(l/2-z)^2}}+\frac{l/2+z}{l\sqrt{R^2+(l/2+z)^2}}\right), \tag{4}$$

where, z is the longitudinal distance to the solenoid center, $\mu_0 = 4\pi \times 10^{-7}$ H/m is the vacuum magnetic permeability, N is the number of coils, I is the coil electric current, l is the length of the solenoid, R is the average radius of the coils. Instead of specifying N and I of the coils, the field is scaled to a specific peak field, B_0, which is optimized to have a uniform field of 0.5 T surrounding the accelerating structures. For this purpose, three types of NC solenoids are assumed with different peak fields:

- Type 0: Solenoid between the AMD and the first accelerating structure. A gap of 2 mm is assumed between the solenoid and the AMD or the structure.
- Type 1: Solenoid surrounding accelerating structures. Each structure is surrounded by 7 solenoids with a total length of 1.38 m and a gap of 20 mm between solenoids. The center of the surrounding solenoids is the same as the structure. Coupler cells of the structure are not surrounded by solenoids.
- Type 2: Solenoid between accelerating structures. A gap of 10 mm is assumed between the solenoid and the structures.

The different types of solenoids are summarized in Table IV. To simplify the design, the solenoids are assumed to have the same length and aperture. The optimized layout of the NC solenoids, as well as the target, AMD and accelerating structures, is displayed in Fig. 9. The total on-axis magnetic field of the AMD and the NC solenoids is presented in Fig. 10.

TABLE IV. NC solenoids for the PIL.

Parameter	Symbol	Unit	Type 0	Type 1	Type 2
Average radius	R	mm	200	200	200
Length	l	mm	180	180	180
Peak field	B_0	T	0.38	0.23	0.31

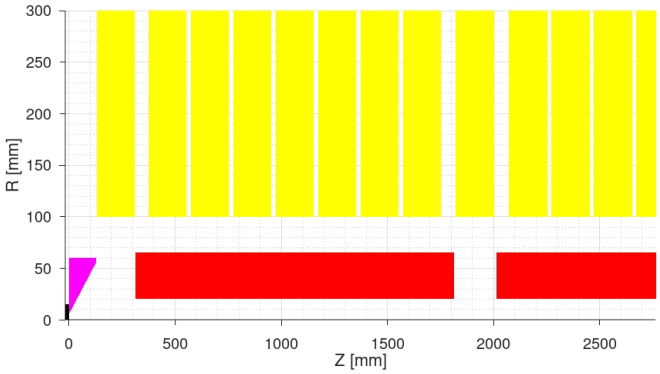

FIG. 9. Cross-sectional view of the schematic layout of the NC solenoids (in yellow), as well as the target (in black), AMD (in cyan) and accelerating structures (in red). Plot ranges are limited for a better display.

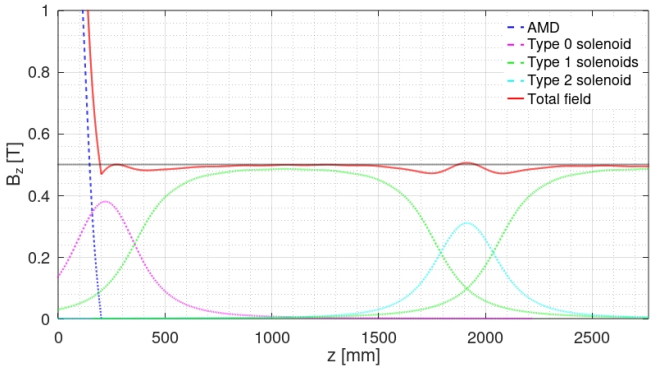

FIG. 10. Total on-axis magnetic field of the AMD and the NC solenoids. A breakdown of the total field is also displayed. Plot ranges are limited for a better display.

E. Collimation-Chicane

In the old studies, the collimation of electrons and photons from the target has never been studied and simulated. In the new simulations, we use a chicane with a collimator placed at the center of the chicane to remove the electrons and photons, based on the SuperKEKB positron chicane design [17]. RF-Track [11, 12] is used to simulate the dipoles in the chicane, assuming a uniform vertical dipole magnetic field. The chicane is composed of four identical dipoles, with only different field directions. The horizontal aperture should be large enough to accommodate the beam with a large horizontal offset and beam size in the bending dipoles. The vertical aperture is usually much smaller limited by the dipole yokes. Therefore, the beam pipe is assumed to have a rectangular aperture shape. The beam pipe aperture is a bit larger at the center of the chicane than inside the dipoles, to make space for the collimator. The chicane parameters, as well as the collimator parameters, are summarized in Table V. The layout of the chicane and the collimator is displayed in Fig. 11.

F. Injector Linac

The Injector Linac (IL) is supposed to accelerate the positrons, as well as the electrons, from 200 MeV to 2.86 GeV. An existed design of the IL [5] is used in the study. The schematic layout is presented in Fig. 12. The IL is composed of five FODO lattice sections, with increasing focusing lengths. The total number of quadrupoles used is 143, including 16 quadrupoles used in the five matching sections. The same "CLIC L-

TABLE V. Chicane and collimator parameters.

Parameter	Symbol	Unit	Value
Chicane			
Dipole length	l	mm	200
Reference energy	e_0	MeV	200
Bending angle	θ	°	4.8, -4.8, -4.8, 4.8
Beam pipe aperture inside dipoles (total width)	D_x, D_y	mm	120, 50
Beam pipe aperture for collimator (total width)	D_x, D_y	mm	180, 60
Distance between chicane and other sections	d_0, d_4	mm	200, 200
Distance between dipoles	d_1, d_2, d_3	mm	160, 250, 160
Collimator			
Collimator length	l	mm	120
Offset of the aperture	x_0	mm	-30
Aperture (total width)	D_x, D_y	mm	60, 60

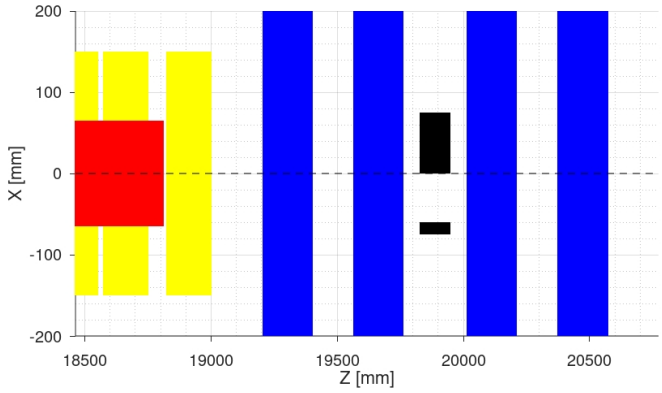

FIG. 11. Cross-sectional view in the Z-X plane of the schematic layout of the chicane dipoles (in blue) and the collimator (in black), as well as the upstream accelerating structures (in red) and NC solenoids (in yellow).

band" structure as the PIL is used. RF-Track [11, 12] is used to simulate the transport of positrons in the IL. The parameters of the FODO lattices are summarized in Table VI. The parameters of the RF accelerating structures that are common in all sections are summarized in Table VII. To simplify the design, the same RF gradient and phase are assumed for all RF structures. The matching sections, as well as the RF gradients and phases are optimized for maximum PDR accepted positron yield.

G. Summary

A brief summary of the improvements in the design and simulation of the CLIC positron source compared with the old studies is as follows:

- Target: The old hybrid target scheme is replaced with a new single target scheme with an optimized target thickness. As a result, the final positron yield is significantly increased and the deposited power is also significantly reduced.
- Primary electrons: The electron beam spot size has been optimized to achieve the maximum final positron yield below the required PEDD limit. As a result of yield improvement, the required electron bunch charge and beam power, inversely proportional to the final positron yield, are also significantly reduced.
- AMD: The old analytic field using the adiabatic formula is replaced with a realistic field from the realistic FC design. Positron yield overestimation in the old simulations with large AMD aperture is solved by using real aperture.
- NC solenoid: Constant on-axis field is replaced with analytic field from a more realistic design of the layout using three different types of solenoids.
- Collimation: A chicane of four dipoles with a collimator placed at the center of the chicane is designed and used to collimate the electrons and photons from the target, which has never been studied before.

III. NOMINAL PERFORMANCE

The final results of the "full simulation" are summarized in Table VIII. Collective effects including the space charge and short-range wakefield are also considered in the simulation. The longitudinal phase spaces of the "full simulation" at the PDR entrance at the 380 GeV energy stage for the DBA acceleration mode are presented in Fig. 13. Compared with the "fast simulation", although a loss of ∼12% is found in the PDR accepted positron yield with the "full simulation", these are the best and most realistic simulation results that have ever been achieved for the CLIC positron source, as already discussed in Section II. Finally, a PDR accepted positron yield of ∼1.8 is achieved at the 380 GeV energy stage, and ∼2.4 is achieved at higher energy stages. The PEDD in target is well controlled below 35 J/g. The required primary electron bunch charges are ∼0.6 nC and ∼0.3 nC

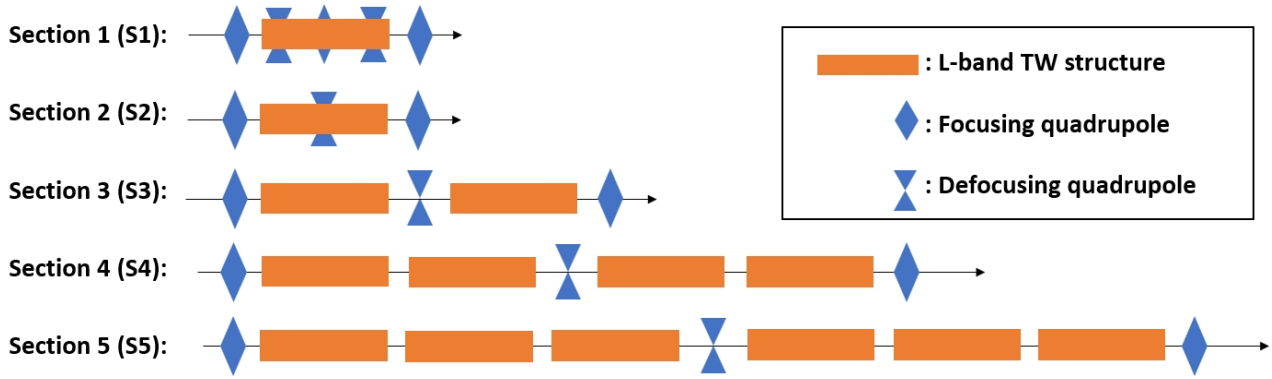

FIG. 12. Schematic layout of IL in five sections.

TABLE VI. FODO lattice parameters of the IL in five sections (S1-S5).

Parameter	Symbol	Unit	S1	S2	S3	S4	S5
Total FODO cells	N_{FODO}		16	18	14	7	6
FODO lattice phase advance	μ	°	90	90	90	90	90
Total quadrupoles	N_{Q}		33	37	29	15	13
Quadrupole length	l_{Q}	m	0.4	0.4	0.4	0.4	0.4
Spacing between quadrupoles	d	m	0.15	0.64	1.65	3.15	4.90
Quadrupoles surrounding a RF structure	n_{Q}		3	1	0	0	0
Total RF structures	N_{RF}		8	18	28	28	36

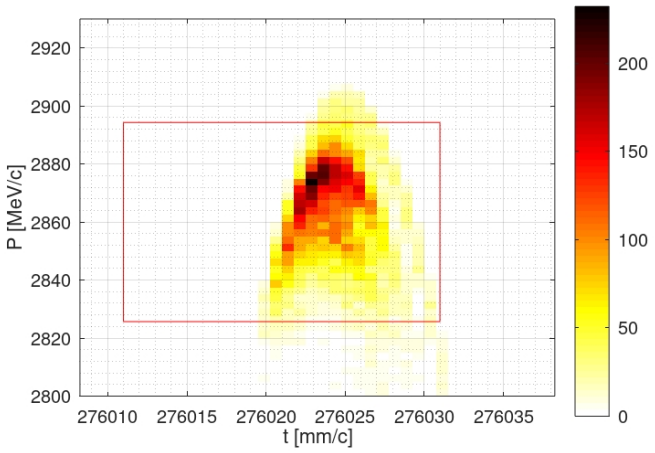

FIG. 13. Longitudinal phase spaces of the "full simulation" at the PDR entrance at the 380 GeV energy stage for the DBA acceleration mode. The PDR acceptance cuts are also displayed.

at 380 GeV and higher energy stages respectively, which are significantly smaller than the nominal bunch charge in the main linac, allowing for a possibility to reduce the electron beam energy, that is studied as an alternative option, as will be discussed in Section V.

IV. MISALIGNMENTS

The misalignment of the CLIC positron source has never been studied before, therefore it is important to look at the impact on the final performance. The misalignments considered in the study are summarized in Table IX. All errors are given as RMS values. A position error of 100 μm and an angular error of 100 μrad are assumed for all RF structures and magnets including the AMD, except for solenoids and dipoles that are short and more difficult to be aligned, in which case an angular error of 200 μrad is assumed. A strength error of 0.1% is assumed for all magnets. A gradient error of 1% and phase error of 0.1° are assumed for all RF structures. Besides, the positron beam from the target is assumed to have a position jitter error of 100 μm and an angular jitter error of 100 μrad.

The PDR accepted positron yield of the "full simulation" for 100 randomly misaligned machines at the 380 GeV energy stage for the DBA acceleration mode is presented in Fig. 14. Compared with the positron yield of the perfect machine without misalignments, the average yield of the misaligned machines is reduced by less than 6%, which is thought to be acceptable. Beam-based alignment corrections are not absolutely necessary but can be done to reduce the losses. Similarly, the normalized horizontal and vertical emittances are presented in Fig. 15 and Fig. 16, respectively. The average emittances are also increased by less than 6%, which is acceptable.

TABLE VII. Common RF structure parameters of the IL.

Parameter	Symbol	Unit	Value
RF frequency	f	GHz	2
RF structure length	l	m	1.5
RF structure aperture (radius)	a_0	mm	20
RF average gradient without compensation	G	MV/m	15.12
RF average gradient with compensation for short-range wakefield	G	MV/m	15.19
RF phase	φ	°	0

TABLE VIII. Final results of the "full simulation" at different energy stages for different acceleration modes (DBA: drive beam-based acceleration; KBA: klystron-based acceleration).

Parameter	Unit	380 GeV		1.5 & 3 TeV
Acceleration mode		DBA	KBA	DBA
Optimized electron beam spot size	mm	2.40	2.45	1.50
Positron yield accepted by PDR		1.78	1.74	2.36
Required electron bunch charge	nC	0.56	0.43	0.30
Electron bunch charge assumed for collective effects	nC	0.8	0.6	0.4
Normalized electron beam power	kW	49.4	51.8	23.5
Normalized PEDD in target	J/g	33.1	33.2	32.8
Normalized total deposited power in target	kW	13.3	13.9	6.3

TABLE IX. Misalignments considered in the study. RMS values are reported.

Misalignment	Unit	Value
Positron error for all elements	μm	100
Angular error for solenoids and dipoles	μrad	200
Angular error for other elements	μrad	100
Strength error for all magnets	%	0.1
RF gradient error for all structures	%	1
RF phase error for all structures	°	0.1
Beam position jitter error	μm	100
Beam angular jitter error	μrad	100

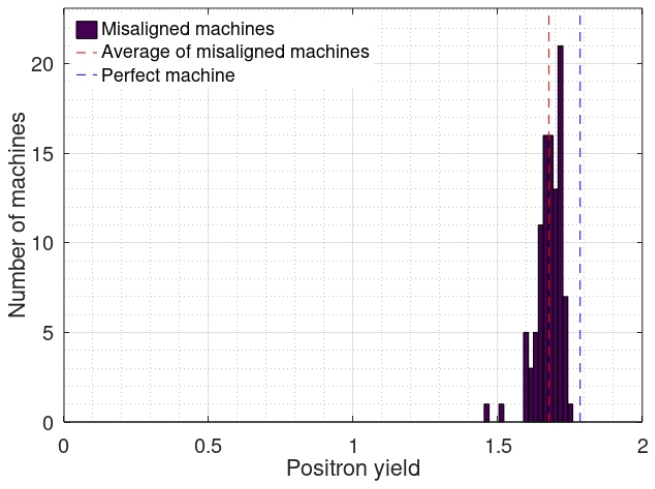

FIG. 14. PDR accepted positron yield of the "full simulation" for 100 randomly misaligned machines at the 380 GeV energy stage for the DBA acceleration mode.

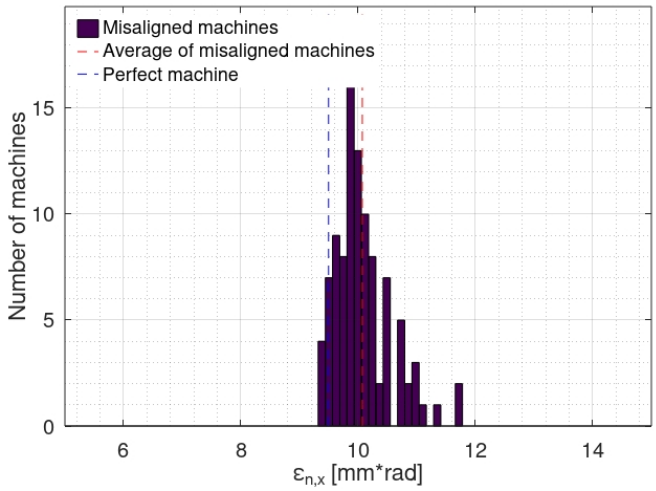

FIG. 15. Normalized horizontal emittance at the PDR entrance of the "full simulation" for 100 randomly misaligned machines at the 380 GeV energy stage for the DBA acceleration mode.

V. REDUCED ELECTRON BEAM ENERGY

It is obvious that a lower electron beam energy would reduce the linac length for the electron beam and the construction cost. The only problem is that the positron yield would also be reduced almost linearly, and a larger bunch charge would be required. In the baseline design, a 5 GeV electron beam is assumed, with a required bunch charge of the electron beam less than 0.6 nC, as seen in Table VIII. It seems possible to reduce the electron beam energy with a larger bunch charge. Therefore, a scan of

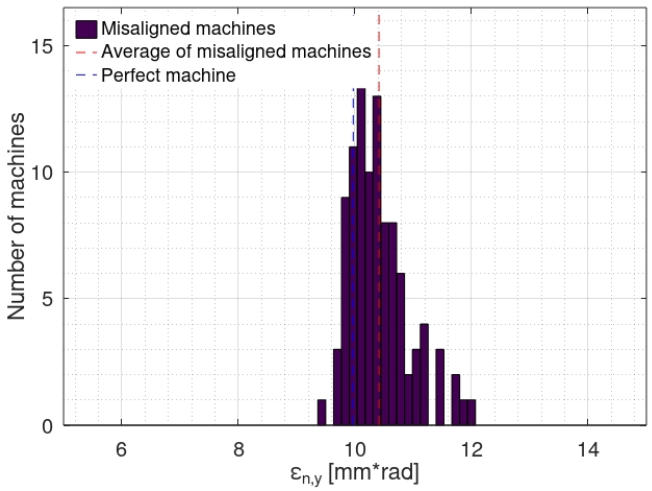

FIG. 16. Normalized vertical emittance at the PDR entrance of the "full simulation" for 100 randomly misaligned machines at the 380 GeV energy stage for the DBA acceleration mode.

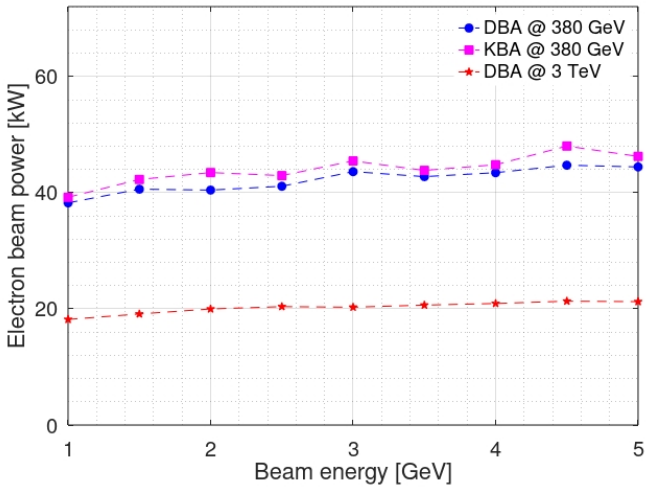

FIG. 18. Normalized electron beam power as a function of the electron beam energy at different energy stages for different acceleration modes.

the electron beam energy is performed to find the minimum energy. For each energy, the target thickness and the electron spot size are optimized separately.As a result, the required bunch charge, normalized beam power and total deposited power in the target are then plotted as a function of the electron beam energy at different energy stages for different acceleration modes, as presented in Figs. 17–19. The normalized beam power and total

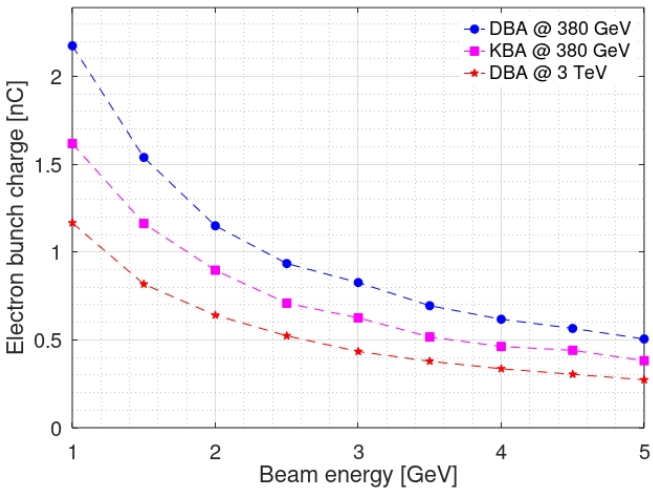

FIG. 17. Required primary electron bunch charge as a function of the electron beam energy at different energy stages for different acceleration modes.

deposited power in the target are both reduced slightly with a reduced electron beam energy. The cooling of the target is also thought to be easier with a lower total deposited power. The operation cost of the electron linac is expected to be reduced

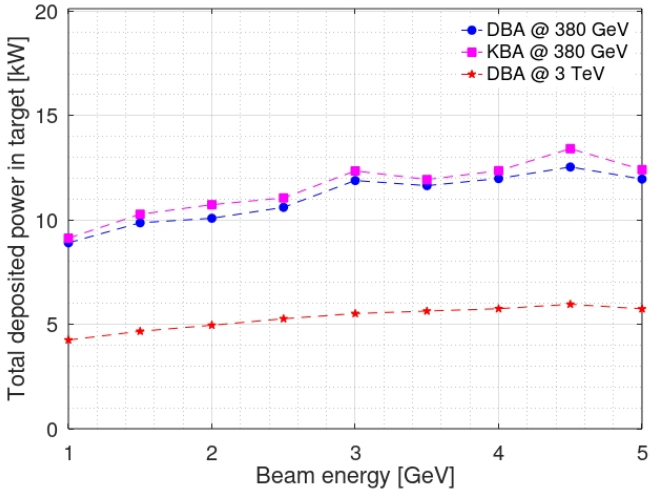

FIG. 19. Normalized total deposited power in the target as a function of the electron beam energy at different energy stages for different acceleration modes.

with the beam energy. Therefore, it seems that the lower the electron beam energy, the better it is in cost saving and target cooling. However, the required electron bunch charge is increased significantly with a reduced beam energy. Finally, it becomes a question of how much bunch charge can be accelerated with good beam quality in the electron linac. A good alternative option for the electron beam energy might be 2.3 GeV, which corresponds to a bunch charge of ∼1 nC. Compared with the 5 GeV baseline, 2.3 GeV beam energy features: a shorter linac length, by a factor $\sim 5/2.3 \sim 2.2$; a beam power reduced by ∼10%, and a total deposited power in target reduced by 12.5%, as can be seen in the figures mentioned above. Nevertheless, this is a preliminary study of the possibility to reduce the energy, and more detailed studies are

necessary if this proposal is to be achieved.

VI. CONCLUSIONS

The baseline design of the CLIC positron source has been updated with a start-to-end optimization at all collision energy stages, for both the drive beam-based and the klystron-based acceleration modes. In the optimized baseline, the hybrid target is replaced with a single amorphous tungsten target with the target thickness and electron spot size optimized. As a result, the final positron yield is significantly increased, and the electron bunch charge and beam power are significantly reduced. Compared with the most recently published optimization in 2019, the positron yield has been improved by a factor of 1.65, enabling the same reduction in the bunch charge and beam power of the primary electron beam. The total deposited power in the target is reduced by a factor of 2.1. The design, cooling, manufacturing and mounting of the target will also be much easier and conservative. Final results of the most realistic simulations to date for the CLIC positron source are presented for the nominal configurations. In this case, the PDR accepted positron yield is about 1.8 for the first stage and 2.4 for higher energy stages, for a drive beam-based acceleration. The required electron bunch charge is about 0.6 nC and 0.3 nC correspondingly, while the electron beam power is about 49 kW and 24 kW. The impact of the misalignments and beam jitters is very important but has never been studied. In our simulations, it is found to be small and certainly acceptable. The average reduction in positron yield of 100 randomly misaligned machines with a jittered beam is less than 6%, while the average emittance growth is also less than 6%. Preliminary investigation of reducing the electron beam energy is presented. The optimization of the electron beam energy becomes a question of how much bunch charge can be accelerated with good beam quality in the electron linac. A good alternative option for the electron beam energy might be 2.3 GeV, which corresponds to a bunch charge of $\sim$1 nC, and features shorter linac length, lower beam power and lower total deposited power in target, compared with the 5 GeV baseline. The construction and operation costs are therefore expected to be reduced accordingly with a shorter linac and a lower beam power. The cooling of the target is also expected to be easier with a lower total deposited power in target.

[1] M. Aicheler, P. Burrows, M. Draper, T. Garvey, P. Lebrun, K. Peach, N. Phinney, H. Schmickler, D. Schulte, and N. Toge, *A Multi-TeV Linear Collider Based on CLIC Technology: CLIC Conceptual Design Report*, CERN Yellow Reports: Monographs (CERN, Geneva, 2012).

[2] M. Aicheler, P. Burrows, N. Catalan Lasheras, R. Corsini, M. Draper, J. Osborne, D. Schulte, S. Stapnes, and M. Stuart (CLICAccelerator), *The Compact Linear Collider (CLIC) – Project Implementation Plan*, edited by M. Aicheler, CERN Yellow Reports: Monographs (2018) 247 p.

[3] H. Bajas, S. Doebert, A. Latina, and Y. Zhao, Flux concentrator optimization for future positron sources, IEEE Transactions on Applied Superconductivity **32**, 1 (2022).

[4] E. Darvish Roknabadi and S. Döbert, TW-Structure Design and E-Field Study for CLIC Booster Linac, , THPOR037 (2016).

[5] C. Bayar, A. K. Ciftci, S. Doebert, and A. Latina, Design and optimisation of the positron production chain for CLIC from the target to the damping ring, Nucl. Instrum. Methods Phys. Res., A **869**, 56 (2017).

[6] S. A. et al., Geant4—a simulation toolkit, Nucl. Instrum. Methods Phys. Res. A **506**, 250 (2003).

[7] J. A. et al., Geant4 developments and applications, IEEE Trans. Nucl. Sci. **53**, 270 (2006).

[8] J. A. et al., Recent developments in geant4, Nucl. Instrum. Methods Phys. Res. A **835**, 186 (2016).

[9] A. Xavier, A simulation code for channeling radiation by ultrarelativistic electrons or positrons, Nuclear Instruments and Methods in Physics Research Section B: Beam Interactions with Materials and Atoms **48**, 278 (1990).

[10] Y. Zhao, A. Latina, S. Doebert, D. Schulte, and L. Ma, *Optimisation of the CLIC positron source at the 1.5 TeV and 3 TeV stages*, Tech. Rep. (CERN, Geneva, 2020).

[11] A. Latina, *RF-Track Reference Manual*, Tech. Rep. (CERN, Geneva, Switzerland, 2021).

[12] A. Latina, The Tracking Code RF-Track and Its Application, JACoW HB **2023**, 245 (2024).

[13] Y. L. Han, C. Bayar, A. Latina, S. Doebert, D. Schulte, and L. L. Ma, Optimization of the CLIC positron source using a start-to-end simulation approach involving multiple simulation codes, Nucl. Instrum. Methods Phys. Res., A **928**, 83 (2019).

[14] R. Chehab, G. Le Meur, B. Mouton, and M. Renard, An adiabatic matching device for the orsay linear positron accelerator, IEEE Transactions on Nuclear Science **30**, 2850 (1983).

[15] A. Kulikov, S. Ecklund, and E. Reuter, Slc positron source pulsed flux concentrator, in *Conference Record of the 1991 IEEE Particle Accelerator Conference* (1991) pp. 2005–2007 vol.3.

[16] P. Martín-Luna, B. Gimeno, D. González-Iglesias, D. Esperante, C. Blanch, N. Fuster-Martínez, P. Martinez-Reviriego, and J. Fuster, On the magnetic field of a finite solenoid, IEEE Transactions on Magnetics **59**, 1 (2023).

[17] T. Kamitani *et al.*, SuperKEKB Positron Source Construction Status, in *5th International Particle Accelerator Conference* (2014) p. MOPRI004.